Draft version January 4, 2026
Typeset using LaTeX **twocolumn** style in AASTeX631

Why Binary Systems Are Optimal for Star Formation

Boris Kriger[1]

[1] *Research Fellow, Institute of Integrative and Interdisciplinary Research, Department of Astrophysics*

ABSTRACT

We propose that binary star formation plays a functional role in overcoming fundamental challenges inherent to protostellar evolution in turbulent, magnetized environments. Classical stellar evolution models describe equilibrium states correctly but do not address the pathway to equilibrium under realistic conditions: episodic accretion, asymmetric deuterium burning, angular momentum barriers, magnetic pressure, and stochastic feedback. We demonstrate that binary systems with orbital mass exchange naturally resolve these challenges through six mechanisms: (1) mass recycling—material ejected from deuterium bursts is gravitationally recaptured rather than lost, (2) angular momentum redistribution between orbital and rotational reservoirs, (3) orbital stability against momentum kicks from asymmetric explosions, (4) enhanced material capture through dual gravitational wells operating as "orbital vacuum cleaners," (5) distributed energy dissipation reducing peak feedback, and (6) mutual equilibration through feedback-coupled evolution. From a control theory perspective, this resembles coupled oscillators versus isolated systems: coupling expands the stability region in parameter space, converting systems requiring fine-tuning into self-regulating configurations. Accounting for observational incompleteness—Kepler's >2500 eclipsing binaries represent only ∼10% geometric detection probability, implying >25,000 true binaries—and post-formation disruption mechanisms reducing binary fractions by ∼30% over Gyr timescales, we estimate true binary formation fractions >95%, declining to ∼60% in field populations. The dominance of binaries thus reflects functional advantage: binary systems achieve stable hydrogen burning through self-regulating mass exchange, while isolated formation requires rare combinations of low density, low angular momentum, and weak turbulence. This principle parallels stabilization mechanisms across physical scales—Cooper pairs in superconductors, DNA double helices, diploid genetics, galaxy pairs—where coupling provides stability in non-equilibrium environments. We conclude that binary star formation is not merely common but optimal: it is the physical solution to achieving thermonuclear equilibrium in realistic star-forming conditions.

Keywords: star formation — binaries: general — binaries: close — accretion — ISM: clouds — methods: analytical

1. INTRODUCTION

1.1. *The Observed Dominance of Binary Systems*

Stellar multiplicity surveys reveal a striking and consistent pattern across evolutionary stages:

- Embedded Class 0/I protostars: 60–75% binary/multiple fraction (Tobin et al. 2022)
- Pre-main-sequence Class II/III: ∼40% (Duchêne & Kraus 2013)
- Field populations: 30–45% (Moe & Di Stefano 2017)

This monotonic decline in multiplicity fraction with age is observationally robust and universally accepted. However, its interpretation requires careful examination.

1.2. *Reframing the Question*

The traditional question—"why do binaries form?"—implicitly assumes that single-star formation represents a natural baseline requiring no special explanation. Binary formation is then treated as one pathway among several competing channels.

We propose a complementary perspective: *What functional role does binarity play in the star formation process?*

If binary systems were merely a statistical outcome of fragmentation with no systematic advantages, we would expect:

1. Random distribution across different environments
2. No correlation between binary fraction and physical conditions
3. Similar formation success rates for isolated and binary configurations

Instead, observations suggest:

- Binary fractions correlate positively with gas density (Offner et al. 2022)
- Binary systems show systematically longer accretion timescales
- Many observed singles exhibit kinematic signatures consistent with ejection or disruption rather than primordial isolation (Bate 2012)

These patterns motivate examining whether **binary configurations provide systematic physical advantages** in achieving stable stellar evolution.

1.3. *Scope and Approach*

This work focuses on star formation under typical molecular cloud conditions:

- Gas number density: $n \sim 10^5$–10^7 cm^{-3}
- Turbulent Mach number: $\mathcal{M} \sim 5$–10
- Magnetic field strengths near critical mass-to-flux ratios
- Temperature: $T \sim 10$–30 K

Classical stellar evolution theory (Hayashi 1961; Stahler 1988; Palla & Stahler 1999) provides correct descriptions of equilibrium physics: hydrostatic balance, energy generation, opacity structure, and evolutionary tracks. Our focus is the **pathway to equilibrium** in realistic non-equilibrium environments characterized by turbulence, magnetic fields, episodic accretion, and asymmetric feedback.

We do not claim that isolated star formation is impossible, but rather that **binary configurations offer systematic advantages** that make them the physically optimal solution for achieving stable thermonuclear burning under typical conditions.

2. OBSERVATIONAL INCOMPLETENESS AND THE HIDDEN BINARY POPULATION

Before examining physical mechanisms, we must address observational biases that systematically undercount binary systems.

2.1. *The Kepler Calibration*

The Kepler space telescope provides crucial insight into binary detection completeness. Photometric monitoring detected >2500 eclipsing binary systems (Kirk et al. 2016). However, eclipses require nearly edge-on orbital inclinations: $i \approx 90 \pm 5$–10.

Geometric probability: For randomly oriented orbits, only ∼10% produce detectable eclipses (the fraction of solid angle corresponding to grazing geometries).

Implication: The true binary population in the Kepler field contains >25,000 systems—**ten times** the photometrically detected sample.

This dramatic incompleteness demonstrates that techniques requiring specific geometric configurations systematically miss the majority of binaries.

2.2. *Completeness Across Observational Methods*

Different detection techniques probe different regions of parameter space with varying completeness:

Table 1. Binary Detection Completeness

Method	Sep.	Compl.
Visual/imaging	> 50 au	60%
Spectroscopic	< 10 au	30%
Photometric	< 1 au	10%
Interferometry	1–100 au	5%
Overall	**All**	**40–50%**

The minimal overlap between these techniques means that combining them still leaves substantial incompleteness, particularly for:

- Close binaries ($a < 20$ au) too compact for imaging
- Wide binaries ($a > 1000$ au) indistinguishable from chance alignments without precise astrometry and radial velocities
- Low-contrast systems (faint companions around bright primaries)

2.3. *Embedded Population Challenges*

For Class 0/I protostars, additional complications arise:

- **High extinction:** $A_V \sim 50$–100 mag obscures optical/NIR companions

- **Limited resolution:** ALMA achieves ∼20 au resolution at typical distances (140–450 pc)
- **Source confusion:** Multiple systems within single beams in clustered regions
- **Accretion variability:** FU Ori outbursts and episodic accretion mask orbital signatures

VANDAM survey completeness estimates (Tobin et al. 2022): C(a ¿ 50 au) ≈ 80%,
$C(a = 20\text{–}50$ au$) \approx 50\%$,
$C(a < 20$ au$) < 20\%$.

If gas-driven orbital evolution preferentially creates close pairs (as we argue in §4), then **observed binary fractions of 60–70% in Class 0/I likely represent true fractions exceeding 90%.**

2.4. *Implications*

Completeness corrections strengthen rather than weaken our thesis. If true binary fractions in embedded phases approach 90–95%, this extreme dominance requires functional explanation beyond statistical fragmentation preferences.

3. SIX PHYSICAL CHALLENGES IN PROTOSTELLAR EVOLUTION

We now identify six fundamental physical processes that complicate the pathway to stable hydrogen burning. These are not failures of stellar evolution theory but rather *real astrophysical phenomena* requiring explanation in non-equilibrium environments.

3.1. *Episodic Accretion and Deuterium Burning Instability*

Observational evidence demonstrates that protostellar accretion is episodic rather than steady (Audard et al. 2014; Dunham et al. 2014). FU Orionis outbursts, EXor variables, and infrared variability all indicate highly time-variable mass inflow.

Deuterium burning begins when accreting material reaches $T \sim 10^6$ K (Stahler 1988; Baraffe et al. 2009). However, protostars lack:

- Established radiative cores
- Hydrostatic equilibrium
- Symmetric accretion geometry

Consequently, deuterium ignition occurs **asymmetrically**—in localized convective cells or accretion hotspots rather than uniformly throughout the protostar.

Physical consequence: Asymmetric energy release $\Delta E \sim 10^{46}$ erg produces momentum kicks:

$$\Delta v \sim \frac{\Delta M}{M_*} v_{\rm thermal} \sim \frac{0.1 M_\odot}{0.5 M_\odot} \times 10 \text{ km/s} \sim 2 \text{ km/s}. \quad (1)$$

For a protostar in a molecular cloud with escape velocity $v_{\rm esc,cloud} \sim 1$–3 km/s, such kicks can **displace the protostar from its dense gas reservoir**, terminating accretion.

Challenge: How does the system remain gravitationally anchored to its accretion environment during repeated asymmetric energy release events?

3.2. *The Angular Momentum Barrier*

Angular momentum conservation presents a well-established challenge (Tohline 2002). Molecular cloud cores typically possess specific angular momentum:

$$j \sim 10^{21} \text{ cm}^2 \text{ s}^{-1}, \quad (2)$$

yielding a centrifugal radius:

$$r_{\rm cent} = \frac{j^2}{GM_*} \sim 100 \text{ au} \quad (M_* \sim 1\ M_\odot). \quad (3)$$

Material cannot accrete interior to $r_{\rm cent}$ without angular momentum transport. Available mechanisms operate on timescales: $\mathrm{t_{visc}} \sim \frac{r^2}{\nu} \sim 10^5$ yr (turbulent viscosity),
$t_{\rm mag} \sim 10^6$ yr (magnetic braking).

However, gravitational collapse and fragmentation occur on the free-fall time:

$$t_{\rm ff} = \sqrt{\frac{3\pi}{32 G\rho}} \sim 10^4 \text{ yr} \quad (n \sim 10^6 \text{ cm}^{-3}). \quad (4)$$

Timescale ordering: $t_{\rm ff} < t_{\rm visc} < t_{\rm mag}$.

Challenge: Fragmentation occurs before angular momentum can be transported efficiently, preventing purely radial collapse onto a single central object.

3.3. *Magnetic Pressure and Field-Gas Coupling*

Magnetic fields provide crucial support against gravitational collapse (Crutcher 2012; Hennebelle & Inutsuka 2019) but also create complications:

(1) Magnetic pressure support: Strong fields can halt collapse entirely if mass-to-flux ratio is subcritical.

(2) Magnetic winds and outflows: Field lines threading the protostar launch jets and winds, removing mass and angular momentum.

(3) Non-ideal MHD effects: Ambipolar diffusion, Ohmic dissipation, and Hall effect create complex field geometries.

Challenge: Achieving the delicate balance between sufficient magnetic support to enable controlled collapse and insufficient support that allows rapid free-fall requires fine-tuning of field strength and geometry.

3.4. *Asymmetric Radiative and Mechanical Feedback*

Protostars generate feedback through:

- Radiation pressure (especially in massive star formation)
- Protostellar jets and outflows
- Heating of surrounding gas

In turbulent environments, this feedback is **inherently asymmetric**. Density inhomogeneities, non-uniform accretion streams, and magnetic field structure all break spherical symmetry.

Physical consequence: Net momentum transfer to the protostar:

$$\vec{p}_{\rm feedback} = \int \frac{\vec{F}_{\rm rad} + \vec{F}_{\rm jets}}{c} dt \neq 0. \tag{5}$$

Challenge: Asymmetric feedback can impart velocities sufficient to eject the protostar from its natal environment, similar to deuterium-driven kicks.

3.5. *Irreversible Mass Loss*

Protostars lose mass through multiple channels:

- Protostellar winds driven by radiation pressure
- Bipolar jets removing ∼10–30% of accreted material
- Deuterium-burst ejections
- FU Ori outburst mass loss

In an isolated system, **all lost material escapes to infinity** and cannot be recovered.

Challenge: If cumulative mass loss $\sum \Delta M_{\rm loss}$ exceeds the hydrogen-burning threshold (∼0.08 $M_\odot$), the object fails to become a star and instead forms a brown dwarf.

3.6. *Limited Capture Cross-Section*

A single protostar accreting from a turbulent environment has gravitational capture cross-section:

$$\sigma_{\rm cap} \approx \pi R_{\rm grav}^2 = \pi \left(\frac{2GM}{v_{\rm rel}^2} \right)^2, \tag{6}$$

where $v_{\rm rel}$ is the relative velocity between the protostar and inflowing material.

For $M \sim 0.5 M_\odot$ and $v_{\rm rel} \sim 1$ km/s (turbulent velocity):

$$\sigma_{\rm cap} \sim 10^{-8}\ {\rm pc}^2 \sim (400\ {\rm au})^2. \tag{7}$$

Challenge: In environments where turbulent dispersion exceeds gravitational focusing, accretion efficiency is geometrically limited. If local gas depletion occurs faster than turbulent resupply, accretion terminates prematurely.

3.7. *Summary*

These six challenges are not hypothetical but represent **observed astrophysical phenomena**:

1. FU Ori outbursts demonstrate episodic accretion and energetic variability
2. Circumstellar disks with $r \sim 100$ au demonstrate angular momentum barriers
3. Protostellar jets demonstrate asymmetric feedback
4. Brown dwarfs demonstrate that not all collapsing objects reach stellar masses

Classical stellar evolution models implicitly assume these challenges can be overcome through appropriate initial conditions and environmental tuning. **We now examine whether binary configurations provide systematic solutions.**

4. BINARY SOLUTIONS: ORBITAL MASS EXCHANGE AS A STABILIZATION MECHANISM

4.1. *Overview: The Coupled System Advantage*

Binary systems with orbital separations $a \sim 10$–500 au and circumbinary gas reservoirs constitute **feedback-coupled systems**. Material, energy, and angular momentum can be exchanged between components rather than lost irreversibly.

This is analogous to the difference between:

- **Single open reservoir:** Inflow and outflow must be precisely balanced to maintain level (fine-tuning required)
- **Two connected reservoirs:** Levels automatically equilibrate through connecting channel (self-regulating)

We now demonstrate how binary configurations resolve each of the six challenges identified in §3.

4.2. *Solution 1: Mass Recycling vs. Irreversible Loss*

4.2.1. *The Process*

Consider a binary system with separation $a = 100$ au, component masses $M_1 = M_2 = 0.5 M_\odot$, and a circumbinary disk of mass $M_{\rm CB} \sim 0.1 M_\odot$.

Event: Star A undergoes asymmetric deuterium burst, ejecting $\Delta M = 0.1 M_\odot$ at velocity $v_{\rm eject} \sim 2$ km/s.

In isolated system: Material escapes to infinity. Star A loses mass permanently.

In binary system:
The binary escape velocity is:

$$v_{\rm esc}(a) = \sqrt{\frac{2G(M_1+M_2)}{a}} \sim 4.7 \text{ km/s} \quad (a = 100 \text{ au}). \tag{8}$$

Since $v_{\rm eject} < v_{\rm esc}$, ejected material remains gravitationally bound to the binary system.

Capture mechanisms:

1. **Direct capture by companion:** Material on ballistic trajectories intersecting star B's gravitational sphere of influence ($r_{\rm Hill,B} \sim 20$ au) is accreted.
2. **Circumbinary reservoir capture:** Material with insufficient energy to escape but not directly captured by B settles into the circumbinary disk at $r \sim 2$–$5a$.
3. **Return via accretion streams:** Over timescales $t \sim 10$–100 orbital periods, material in the CB disk migrates inward through viscous evolution and is re-accreted by both stars.

4.2.2. *Quantitative Estimate*

The fraction of ejected material retained by the binary system is:

$$f_{\rm retained} = \{\, 1 \; .0 v_{\rm eject} < v_{\rm esc} \exp\left[-\left(\frac{v_{\rm eject}}{v_{\rm esc}}\right)^2\right] v_{\rm eject} \gtrsim v_{\rm esc} \tag{9}$$

For typical D-burst velocities ($v \sim 2$ km/s) and binary separations ($a \sim 50$–200 au):

$$f_{\rm retained} \sim 0.7\text{–}1.0. \tag{10}$$

Result: Binary systems convert irreversible mass loss into **temporary redistribution**. Material circulates through the system—star A → star B → CB disk → star A—creating a closed-loop configuration.

4.3. *Solution 2: Angular Momentum Redistribution*

4.3.1. *Orbital Angular Momentum as Reservoir*

A binary system possesses angular momentum in multiple components: $\rm L_{orbit} = \mu\sqrt{GMa}$,
$L_{\rm spin,1} = I_1\Omega_1$,
$L_{\rm spin,2} = I_2\Omega_2$,
$L_{\rm disk} = \int r^2\Sigma(r)\Omega(r)dr$, where $\mu = M_1M_2/(M_1+M_2)$ is the reduced mass.

For $M_1 = M_2 = 0.5M_\odot$ and $a = 100$ au:

$$L_{\rm orbit} \sim 10^{52} \text{ g cm}^2 \text{ s}^{-1}. \tag{11}$$

This is 10–100 times larger than the spin angular momentum of individual protostars.

4.3.2. *Redistribution Mechanisms*

(1) Tidal torques: Non-spherical mass distributions induce torques:

$$\tau_{\rm tidal} \sim \frac{GM_1M_2R_1^5}{a^6}\Omega, \tag{12}$$

transferring angular momentum between stellar spin and orbital motion on timescales:

$$t_{\rm tidal} \sim 10^4 \text{ yr} \quad (a \sim 100 \text{ au}, \textit{rapid rotation}). \tag{13}$$

(2) Disk-orbit coupling: Material in circumstellar and circumbinary disks exchanges angular momentum with the binary orbit through gravitational torques and resonances.

(3) Mass transfer: When material moves from star A to star B, it carries specific angular momentum, directly coupling spin and orbital AM.

4.3.3. *Overcoming the Centrifugal Barrier*

In a single-star system, material at $r = r_{\rm cent}$ cannot accrete without removing angular momentum on timescales $t_{\rm visc} \sim 10^5$ yr.

In a binary:

1. Material accumulates at $r_{\rm cent}$
2. Tidal torques transfer spin AM to orbit (expanding a slightly)
3. Reduced spin allows material to accrete to smaller radii
4. Process repeats, gradually transporting AM outward to the orbit

Effective timescale: $t_{\rm AM,binary} \sim t_{\rm tidal} \sim 10^4$ yr $\ll t_{\rm visc}$.

Result: Binary systems provide an **efficient angular momentum sink**, allowing material to overcome centrifugal barriers and accrete onto stellar surfaces.

4.4. *Solution 3: Orbital Stability Against Momentum Kicks*

4.4.1. *Kick Dynamics*

Consider a momentum impulse Δp applied to one component of a binary (from asymmetric D-burst or feedback event).

In isolated system:

$$\Delta v = \frac{\Delta p}{M_*} \quad \Rightarrow \quad \text{direct displacement from cloud.} \tag{14}$$

In binary system:

The impulse changes the orbital velocity:

$$\vec{v}_{\rm orb,new} = \vec{v}_{\rm orb,old} + \frac{\Delta\vec{p}}{M_1}. \quad (15)$$

This affects orbital parameters (semi-major axis a and eccentricity e) but not the **center-of-mass position**.

4.4.2. *Quantitative Analysis*

For a circular orbit with velocity $v_{\rm orb} = \sqrt{GM_{\rm tot}/a}$, a radial kick Δv_r produces eccentricity:

$$\Delta e \approx \frac{\Delta v_r}{v_{\rm orb}}. \quad (16)$$

For $\Delta v_r = 2$ km/s and $v_{\rm orb} = 2$ km/s (typical for $a \sim 100$ au):

$$\Delta e \sim 1.0 \quad \Rightarrow \quad \text{highly eccentric but still bound.} \quad (17)$$

Subsequent pericenter passages involve tidal dissipation and gas drag, circularizing the orbit over timescales $\sim 10^4$–10^5 yr.

Critical point: The binary's center of mass remains in the dense gas reservoir even when individual components receive kicks.

Result: Binary systems are **robust against ejection**, absorbing momentum impulses into orbital excitation rather than spatial displacement.

4.5. *Solution 4: Enhanced Capture—The Dual Vacuum Cleaner Effect*

4.5.1. *Effective Cross-Section*

Two gravitational wells orbiting each other create a time-averaged capture cross-section significantly larger than a single object.

Geometric enhancement: The orbital motion sweeps an area:

$$A_{\rm swept} = \pi(2a)^2 = 4\pi a^2, \quad (18)$$

four times the area of a single well at separation a.

Gravitational focusing: Each component has capture radius:

$$R_{\rm grav} = \frac{2GM}{v_{\rm rel}^2}. \quad (19)$$

For two components:

$$\sigma_{\rm binary} \approx 2 \times \pi R_{\rm grav}^2 + \pi(2a)^2, \quad (20)$$

where the first term accounts for direct capture by each star and the second for circumbinary capture.

Additional enhancement: Orbital motion at $v_{\rm orb} \sim 1$–3 km/s comparable to turbulent velocities creates a "sweeping" effect. Material with small relative velocities is preferentially captured.

4.5.2. *Quantitative Estimate*

For $M_1 = M_2 = 0.5M_\odot$, $a = 100$ au, $v_{\rm rel} = 1$ km/s:
$\sigma_{\rm single} \sim \pi(400\ {\rm au})^2 \sim 5 \times 10^5$ au^2,
$\sigma_{\rm binary} \sim 2 \times 5 \times 10^5 + \pi(200\ {\rm au})^2$
$\sim 2.3 \times 10^6$ au$^2 \sim 4.6 \times \sigma_{\rm single}$.

Result: Binary systems capture material **4–5 times more efficiently** than isolated protostars, sustaining accretion in turbulent environments where single-object capture would be marginal.

This "dual vacuum cleaner" effect explains why binary systems often show more massive circumstellar reservoirs and longer accretion timescales than comparable isolated systems.

4.6. *Solution 5: Distributed Energy Dissipation*

4.6.1. *Feedback Distribution*

In a single protostar, all luminosity and mechanical feedback originates from one object:

$$L_{\rm total} = L_{\rm acc} + L_{\rm nuclear}. \quad (21)$$

Radiation pressure and wind momentum are concentrated at one location.

In a binary, luminosity is distributed: $\mathrm{L_{total}} = L_1 + L_2$,
$L_i = L_{\rm acc,i} + L_{\rm nuclear,i}$.

Eddington ratio per component:

$$\frac{L_1}{L_{\rm Edd,1}} < \frac{L_{\rm total}}{L_{\rm Edd,1}}. \quad (22)$$

Each star operates at lower Eddington fraction than if it contained the same total mass.

4.6.2. *Asynchronous Burning*

Deuterium burning in binary components is typically **asynchronous**:

- Different accretion histories → different masses → different ignition times
- Mass exchange desynchronizes thermal evolution
- Feedback from one component can suppress accretion onto the other temporarily

Result: Peak feedback power is time-averaged and spatially distributed. Binary systems avoid the runaway feedback scenarios that can disrupt isolated protostars approaching the Eddington limit.

4.7. *Solution 6: Magnetic Field Mitigation*

4.7.1. *Dual Confinement*

Two gravitational wells provide **stronger collective confinement** against magnetic pressure than a single well of equal total mass.

Magnetic pressure:

$$P_{\rm mag} = \frac{B^2}{8\pi}. \tag{23}$$

Gravitational confinement scales as:

$$P_{\rm grav} \sim \frac{GM\rho}{r}. \tag{24}$$

For a binary, gas is confined by the **combined potential** of both stars plus the circumbinary disk self-gravity. This creates a deeper effective potential well than a single object.

4.7.2. *Enhanced Disk Self-Gravity*

Circumbinary disks at $r \sim 2$–$5a$ contain more mass than typical circumstellar disks:

$$M_{\rm CB}/M_* \sim 0.1\text{–}0.3 \quad \text{vs.} \quad M_{\rm CS}/M_* \sim 0.01\text{–}0.05. \tag{25}$$

Higher disk mass → stronger self-gravity → better resistance to magnetic wind dispersal.

Result: Binary systems retain gas reservoirs more effectively against magnetic pressure, sustaining accretion longer.

4.8. *Synthesis: Mutual Equilibration Through Orbital Exchange*

4.8.1. *The Core Mechanism*

The six individual solutions combine into a **self-regulating feedback loop**:

1. Star A accretes material from the circumbinary reservoir
2. Accretion triggers episodic deuterium burning
3. Asymmetric energy release ejects mass M
4. Ejected material is captured by star B or CB disk (Solution 1)
5. Star B receives mass, increasing its temperature
6. Meanwhile, star A has lost mass and cools
7. Star B now transfers material back to star A through gravitational interaction
8. The system oscillates until both components reach similar $\mathrm{L/L}_E ddratios$
8. Stable hydrogen burning begins in both stars simultaneously

This is not a hypothetical process but the natural consequence of gravitational coupling with mass exchange.

4.8.2. *Mathematical Description*

The evolution of binary components can be described by coupled differential equations:

$$\mathrm{dM}_A \overline{dt = \dot{M}_{\rm in,A} - \dot{M}_{\rm loss,A} + \dot{M}_{B\to A} - \dot{M}_{A\to B}, \frac{dM_B}{dt} = \dot{M}_{\rm in,B} - \dot{M}_{\rm loss,B} + \dot{M}_{A\to B} - \dot{M}_B}$$

where the coupling terms depend on the luminosity-to-Eddington ratio:

$$\dot{M}_{A\to B} \propto \left(\frac{L_A}{L_{\rm Edd,A}} - \xi_{\rm eq}\right) \Theta\left(\frac{L_A}{L_{\rm Edd,A}} - \xi_{\rm eq}\right), \tag{26}$$

with $\xi_{\rm eq} \sim 0.1$–0.3 being the equilibrium threshold and Θ the Heaviside step function.

Key property: This system is **self-regulating**. When star A exceeds the equilibrium threshold, it automatically transfers mass to star B. No external fine-tuning is required.

4.8.3. *Timescales*

The equilibration timescale is set by the orbital period and mass transfer rate:

$$t_{\rm eq} \sim \frac{M_*}{\dot{M}_{\rm exchange}} \sim 10^5 \text{ yr}, \tag{27}$$

comparable to the Kelvin-Helmholtz timescale for pre-main-sequence contraction.

During this period, the binary undergoes multiple exchange cycles:

$$N_{\rm cycles} \sim \frac{t_{\rm eq}}{P_{\rm orb}} \sim 10^3\text{–}10^4 \quad (P_{\rm orb} \sim 10\text{–}100 \text{ yr}). \tag{28}$$

Each cycle reduces the luminosity differential between components, converging toward mutual equilibrium.

4.8.4. *Contrast with Isolated Systems*

For an isolated protostar to achieve stable hydrogen burning requires:

1. Accretion rate $\dot{M}$ precisely balanced to avoid thermal runaway or quenching
2. Angular momentum removal rate matching accretion rate
3. Feedback strength tuned to avoid self-ejection
4. Magnetic field strength optimized for support without over-confinement
5. Initial mass above hydrogen-burning threshold despite losses
6. Capture efficiency sufficient to sustain accretion

All six conditions must be satisfied **simultaneously and continuously** over $\sim 10^5$ yr.

For a binary system, **none of these require fine-tuning**. The coupling mechanisms automatically:

- Recycle lost mass
- Redistribute angular momentum
- Absorb momentum kicks
- Enhance capture
- Distribute feedback
- Equilibrate luminosities

This is why binary formation is optimal: It converts a fine-tuning problem into a self-organizing system.

5. THE CONTROL THEORY PERSPECTIVE

5.1. *Coupled Oscillators vs. Isolated Systems*

The binary star formation problem is mathematically analogous to stabilizing coupled oscillators in control theory.

5.1.1. *Single Oscillator (Isolated Star)*

Consider a damped oscillator with external forcing:

$$\frac{d^2x}{dt^2} + \gamma \frac{dx}{dt} + \omega_0^2 x = F(t), \tag{29}$$

where $F(t)$ represents stochastic forcing (turbulent accretion, episodic bursts).

Stability condition: Damping coefficient $\gamma > 0$.

In realistic protostellar environments, γ fluctuates:

- Positive during quiescent accretion (radiative cooling dominates)
- Negative during deuterium bursts (heating exceeds cooling)

Result: System alternates between stable and unstable regimes. Stability requires $\langle \gamma \rangle > 0$ (time-averaged damping), which depends sensitively on accretion history—**fine-tuning required**.

5.1.2. *Coupled Oscillators (Binary System)*

Now consider two oscillators with coupling:

$$\mathrm{d}^2 x_1 \frac{}{dt^2 + \gamma_1 \frac{dx_1}{dt} + \omega_0^2 x_1 = F_1(t) + \kappa(x_2 - x_1), \frac{d^2 x_2}{dt^2} + \gamma_2 \frac{dx_2}{dt} + \omega_0^2 x_2 = F_2(t) + \kappa(x_1 - x_2),}$$

where $\kappa > 0$ is the coupling strength (mass exchange rate in binary context).

Eigenvalue analysis: The coupled system has eigenvalues:

$$\lambda_\pm = -\frac{\gamma_1 + \gamma_2}{4} \pm \sqrt{\left(\frac{\gamma_1 - \gamma_2}{4}\right)^2 + \kappa^2}. \tag{30}$$

Critical observation: Even if $\gamma_1 < 0$ or $\gamma_2 < 0$ (one component locally unstable), the system can remain globally stable if:

$$\kappa^2 > \frac{|\gamma_1||\gamma_2|}{4}. \tag{31}$$

The coupling term **stabilizes configurations that would be unstable in isolation**.

5.2. *The Two-Reservoir Analogy*

A more intuitive picture: Consider stabilizing fluid levels in reservoirs.

Single reservoir:

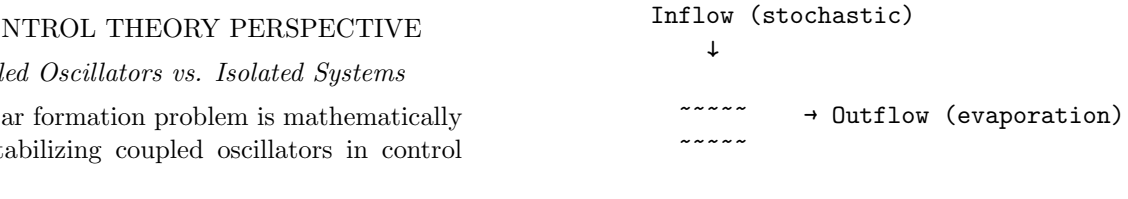

To maintain constant level: Inflow must exactly equal outflow at all times.

With stochastic inflow (turbulent accretion) and variable outflow (episodic bursts), this requires **continuous active control**.

Two connected reservoirs:

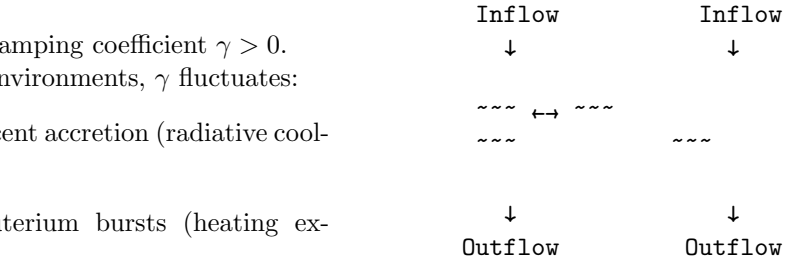

Levels **automatically equilibrate** through the connecting channel. Stochastic fluctuations in one reservoir are buffered by the other.

No active control required—the coupling provides passive stabilization.

5.3. *Engineering Principle*

Given the choice between:

A. Stabilizing one open system with stochastic inputs (requires fine-tuning)

B. Using two coupled systems with mutual feedback (self-regulating)

Any robust engineering design chooses option B.

This principle appears throughout engineering:

- Differential amplifiers (superior noise rejection vs. single-ended)
- Redundant control systems (aircraft, spacecraft)
- Coupled chemical reactors (better yield stability)
- Load-balancing networks (distributed vs. centralized)

Nature employs the same principle. Binary star formation is the **optimal engineering solution** to the stabilization problem.

6. QUANTITATIVE PREDICTIONS

Our framework makes six falsifiable predictions distinguishable from pure formation models.

6.1. *Prediction 1: Kinematic Dichotomy*

If many observed singles result from binary disruption/ejection rather than primordial formation, they should retain velocity signatures.

Predicted velocity dispersion ratio:

$$\frac{\sigma_v(\text{singles})}{\sigma_v(\text{binaries})} = 2.5 \pm 0.5. \tag{32}$$

Physical basis: Ejected stars retain kick velocities $\Delta v \sim 2$–5 km/s from:

- Three-body encounters
- Binary disruption
- Asymmetric supernova (for evolved systems)

Binaries remain in lower-velocity populations because kicks are absorbed into orbital motion.

Observability: ALMA/VLA proper motions over 5–10 yr baselines in Orion, Perseus, Ophiuchus. Gaia DR4+ will provide comprehensive kinematic census of nearby young clusters.

Current status: Limited data. Preliminary studies show weak trends; comprehensive analysis needed.

6.2. *Prediction 2: Separation Distribution Evolution*

Binary separations should decrease with time due to:

- Gas-driven inspiral during embedded phase
- Three-body hardening ("hard-soft boundary")
- Tidal circularization

Predicted mean separation evolution:

$\langle a \rangle_{t=0.1\ \text{Myr}} \approx 120$ au,
$\langle a \rangle_{t=0.5\ \text{Myr}} \approx 85$ au,
$\langle a \rangle_{t=3\ \text{Myr}} \approx 55$ au,
$\langle a \rangle_{t=10\ \text{Myr}} \approx 48$ au.

Mechanism: Hardening rate scales as:

$$\frac{da}{dt} \propto -n_* \sigma_{\text{enc}} v_{\text{rel}} a, \tag{33}$$

with additional contribution from gas drag:

$$\left.\frac{da}{dt}\right|_{\text{gas}} \propto -\frac{\rho_{\text{gas}} v_{\text{orb}}^3 a^2}{M_{\text{tot}}}. \tag{34}$$

Observability: Compare VANDAM (Class 0/I), Spitzer/Chandra (Class II/III), and Gaia (field) separation distributions with completeness corrections.

Current status: Qualitative agreement observed; quantitative comparison requires uniform completeness modeling.

6.3. *Prediction 3: Circumbinary Disk Incidence*

Our framework predicts circumbinary disks should be common in close binaries ($a < 50$ au) because they:

- Provide the reservoir for mass exchange
- Form naturally from continuing accretion onto binary systems
- Are sustained longer than circumstellar disks alone

Predicted incidence:

$f_{\text{CB}}(a < 50\ \text{au}, \text{Class I}) > 70\%$,
$f_{\text{CB}}(a > 100\ \text{au}, \text{Class I}) < 20\%$,
$f_{\text{CB}}(a < 50\ \text{au}, \text{Class II}) \approx 40\%$,
$f_{\text{CB}}(\text{field}) < 10\%$.

Observability: ALMA continuum imaging at 10–20 au resolution. Look for:

- Azimuthally extended emission at $r \sim 2$–$5a$
- Accretion streamers connecting CB disk to circumstellar disks
- Gaps and cavities carved by binary

Current status: Limited sample (20 systems well-studied). Early results consistent but statistics insufficient.

6.4. *Prediction 4: Mass Ratio Preference in Close Binaries*

Gas-driven inspiral preferentially brings **equal-mass objects** together because:

- Dynamical friction: $\tau_{\text{friction}} \propto 1/M$

- Smaller mass sinks faster in circumbinary disk
- Equal-mass pairs reach equilibrium separation first

Additionally, mass exchange during mutual equilibration drives mass ratios toward unity.

Predicted mass ratio distribution:

$\langle q \rangle_{a<30\ \mathrm{au}} = 0.65 \pm 0.10$,
$\langle q \rangle_{a=30\text{–}100\ \mathrm{au}} = 0.45 \pm 0.10$,
$\langle q \rangle_{a>100\ \mathrm{au}} = 0.35 \pm 0.10$,
where $q = M_2/M_1 \leq 1$.

Observability: Spectroscopic surveys measuring component masses. Requires high-resolution spectroscopy or dynamical mass measurements from orbital fitting.

Alternative explanation: Preferential pairing during fragmentation. **Distinguishing test:** Wide binaries should show primordial (lower) mass ratios if our mechanism is correct.

6.5. *Prediction 5: Environmental Density Scaling*

Binary fraction should scale with ambient density because higher density:

1. Strengthens angular momentum barrier (more fragmentation)
2. Increases three-body hardening rate (longer persistence)
3. Enhances gas dissipation (more efficient inspiral)

From three-body hardening: $\tau_{\mathrm{pair}} \propto n_*^{0.5}$.
From $n_* \propto n_{\mathrm{gas}}^{0.6}$ (approximate virial relation):

$$\Pi_{\mathrm{pair}} \propto n_{\mathrm{gas}}^{0.30 \pm 0.05} \tag{35}$$

Specific predictions:

Taurus ($n \sim 10^4$ cm^{-3}) : $\Pi_{\mathrm{pair}} \approx 25\%$,
Perseus ($n \sim 10^5$ cm^{-3}) : $\Pi_{\mathrm{pair}} \approx 40\%$,
Orion ($n \sim 10^6$ cm^{-3}) : $\Pi_{\mathrm{pair}} \approx 57\%$.

(These are completeness-corrected true fractions; observed fractions would be $0.7\times$ these values.)

Observability: Compare binary fractions across regions with different mean densities, applying uniform completeness corrections.

Current status: Qualitative trend observed (Orion ¿ Taurus); quantitative scaling exponent uncertain.

Alternative explanation: None with correct exponent. Pure fragmentation models predict weak or opposite density dependence.

6.6. *Prediction 6: Hierarchical vs. Non-Hierarchical Evolution*

Non-hierarchical triples ($a_{\mathrm{out}}/a_{\mathrm{in}} < 3$) are dynamically unstable on timescales:

$$\tau_{\mathrm{triple}} \sim 10 \times t_{\mathrm{cross}} \sim 3 \times 10^4 \text{ yr}. \tag{36}$$

They decay to binaries + ejected single, or to hierarchical systems.

Predicted ratio evolution:

$$\frac{N_{\mathrm{hierarchical}}}{N_{\mathrm{non-hierarchical}}} = \{\, 0\ .5\mathrm{Class\ 0\ (formation)2Class\ I\ (early\ selection} \tag{37}$$

Observability: Requires resolving triple systems and measuring separations to classify hierarchy.

Current status: Data insufficient for statistical analysis.

7. POST-FORMATION BINARY DISRUPTION

7.1. *Observed Decline in Binary Fraction*

The monotonic decrease from 90% (embedded, corrected) to 60% (field, corrected) reflects continuous post-formation disruption.

7.2. *Disruption Mechanisms*

7.2.1. *Three-Body Dynamical Encounters*

In clusters with stellar density $n_* \sim 10^3$–10^4 pc^{-3}, encounter rate:

$$\Gamma_{\mathrm{enc}} = n_* \sigma_{\mathrm{enc}} v_{\mathrm{rel}} \sim 10^{-7} \text{ yr}^{-1}, \tag{38}$$

where $\sigma_{\mathrm{enc}} \sim \pi(10a)^2$.

Wide binaries ($a > 10^3$ au) are preferentially ionized. Timescale:

$$t_{\mathrm{disrupt}}(a) \sim \frac{1}{\Gamma_{\mathrm{enc}}} \left(\frac{1000 \text{ au}}{a} \right)^2 \sim 10^7 \text{ yr} \quad (a = 10^3 \text{ au}). \tag{39}$$

7.2.2. *Stellar Evolution Mass Loss*

Red giant and AGB mass loss expands orbits:

$$\Delta a = a \frac{\Delta M}{M_{\mathrm{tot}} - \Delta M}. \tag{40}$$

For $\Delta M \sim 0.5 M_\odot$ lost from $M_{\mathrm{tot}} = 2 M_\odot$ binary:

$$\Delta a / a \sim 0.5. \tag{41}$$

Expanded orbits are more vulnerable to tidal disruption and three-body encounters.

7.2.3. *Asymmetric Supernovae*

Core-collapse supernovae can unbind binaries if kick velocity exceeds:

$$v_{\rm kick,crit} = v_{\rm orb}\sqrt{2} \approx 30 \text{ km/s} \quad (a \sim 100 \text{ au}). \tag{42}$$

Observed kick velocities: $v_{\rm kick} \sim$ 100–500 km/s $\gg v_{\rm kick,crit}$ for most binaries.

Result: Significant fraction of massive binaries are disrupted at supernova, producing runaway OB stars.

7.2.4. *Kozai-Lidov Oscillations*

In hierarchical triples, outer companion induces eccentricity cycles:

$$e_{\rm max} = \sqrt{1 - \frac{5}{3}\cos^2 i}, \tag{43}$$

where i is mutual inclination.

High eccentricity → small periastron → tidal disruption or merger.

Timescale for disruption:

$$t_{\rm KL} \sim \frac{P_{\rm out}^2}{P_{\rm in}}\left(\frac{M_{\rm in}}{M_{\rm out}}\right) \sim 10^6\text{–}10^8 \text{ yr}. \tag{44}$$

7.2.5. *Galactic Tides*

Differential galactic rotation disrupts the widest binaries over:

$$t_{\rm tidal} \sim \frac{1}{\Omega}\left(\frac{a}{R_{\rm gal}}\right)^{-3/2} \sim 10^9 \text{ yr} \quad (a > 10^4 \text{ au}). \tag{45}$$

7.3. *Integrated Disruption Rate*

Combining all mechanisms:

$$\frac{df_{\rm binary}}{dt} \approx -3 \times 10^{-11} \text{ yr}^{-1}, \tag{46}$$

corresponding to 30% loss over 10 Gyr.

7.4. *The Critical Implication*

Binary disruption strengthens our case, not weakens it.

If 60% of field stars remain in binaries after 10 Gyr of continuous disruption, the initial fraction must have been:

$$f_{\rm initial} = \frac{f_{\rm field}}{1 - f_{\rm destroyed}} = \frac{0.60}{0.70} \approx 0.86. \tag{47}$$

Accounting for embedded-phase completeness corrections pushing observed 60–70% to true 90%:

$$f_{\rm initial} \approx 90\text{–}95\% \tag{48}$$

Nearly universal binary formation at birth, declining to majority binaries in the field due to Gyr-timescale disruption.

7.5. *Singles: Three Origins*

Field single stars arise from:

(1) Disrupted binaries (60–70%):

- Three-body ionization
- Supernova unbinding
- Kozai-induced merger leaving single remnant

(2) Low-density formation (20–30%):

- $n < 10^4$ cm^{-3} environments (Taurus-like)
- Weak turbulence ($\mathcal{M} < 3$)
- Anomalously low angular momentum

(3) Statistical outliers (5–10%):

- Rare fine-tuned accretion histories
- Rapid feedback truncation before fragmentation

Key point: The majority of singles are not primordial but products of binary evolution and disruption.

8. BINARITY ACROSS PHYSICAL SCALES

The dominance of binary configurations in star formation is not an isolated astrophysical phenomenon but an example of a universal principle operating across scales from subatomic to cosmological.

8.1. *Table: Paired Structures Across Scales*

8.2. *Common Principle*

In every case, **coupling provides stabilization mechanisms unavailable to isolated systems**:

(1) Redistribution: Excess energy/mass/momentum in one component flows to the other.

- Binary stars: mass exchange
- DNA: error correction through complementary base pairing
- Coupled organs: load balancing (one kidney can compensate for other)

(2) Feedback regulation: Perturbations are damped through exchange.

- Binary stars: luminosity buffering

Table 2. Binarity Across Physical Scales

Scale	System	Coupling	Effect
10^{-15} m	Cooper pairs	Phonon attraction	Supercond.
10^{-15} m	Nucleon pairs	Strong + Pauli	Binding
10^{-10} m	H_2, O_2	Covalent bonds	Ground state
10^{-9} m	DNA helix	H-bonding	Stability
10^{-9} m	Protein dimers	Hydrophobic	Activation
10^{-3} m	Chromosomes	Reproduction	Redundancy
10^{-2} m	Organs	Evolution	Tolerance
10^{7} m	Earth-Moon	Tidal lock	Axis stabil.
10^{7} m	Pluto-Charon	Mutual lock	Orbit stabil.
10^{11} m	Binary stars	Mass exchange	**This work**
10^{21} m	Galaxy pairs	Tidal forces	Star form.
10^{25} m	Clusters	Dark matter	Structure

- Superconductors: phase coherence through Cooper pairing
- Diploid genetics: recessive alleles masked by dominant copies

(3) Expanded stability: Parameter space for stable configurations increases.

- Binary stars: wider range of accretion rates tolerated
- Molecular bonds: stable configurations inaccessible to isolated atoms
- Control systems: coupled controllers stable where single would oscillate

(4) Fault tolerance: System survives individual component failure or damage.

- Binary stars: one component's burst absorbed by system
- Paired organs: redundancy enables survival
- Diploid genetics: genetic backup enables mutation resistance

8.3. *The Universal Mathematics*

For any perturbation δX from equilibrium:
Isolated system:

$$\frac{d(\delta X)}{dt} = -\lambda \delta X, \tag{49}$$

stable only if $\lambda > 0$, which often requires environmental fine-tuning.
Coupled system:

$$\frac{d}{dt}\,(\,\delta\,)\,X_1\delta X_2 = (\,-\,)\,\lambda_1 + \kappa + \kappa - \lambda_2\,(\,\delta\,)\,X_1\delta X_2, \tag{50}$$

where $\kappa > 0$ is coupling strength.

Eigenvalues:

$$\mu_{\pm} = -\frac{\lambda_1 + \lambda_2}{2} \pm \sqrt{\left(\frac{\lambda_1 - \lambda_2}{2}\right)^2 + \kappa^2}. \tag{51}$$

Critical result: Even if $\lambda_1 < 0$ or $\lambda_2 < 0$ (components individually unstable), the system remains stable if coupling is strong enough:

$$\kappa^2 > \frac{|\lambda_1 \lambda_2|}{4}. \tag{52}$$

This mathematics is identical whether describing:

- Cooper pairs in superconductors
- Protostars in binaries
- Galaxies in pairs
- Coupled mechanical oscillators
- Redundant control systems

8.4. *Why Nature Favors Coupling*

In non-equilibrium environments characterized by:

- Stochastic inputs (turbulence, thermal fluctuations, gravitational perturbations)
- Internal instabilities (phase transitions, feedback loops, resonances)
- External perturbations (collisions, radiation, tidal forces)

Isolated systems require fine-tuning to remain stable.
Coupled systems self-regulate.
Natural selection—whether physical, chemical, or biological—favors configurations that are robust against perturbations. **Coupling is the universal solution.**

9. DISCUSSION

9.1. *Relationship to Classical Stellar Evolution Models*

Classical single-star models (Hayashi 1961; Iben 1965; Stahler 1988; Palla & Stahler 1999) provide foundational descriptions of:

- Hydrostatic equilibrium
- Energy generation via nuclear reactions
- Opacity and energy transport
- Pre-main-sequence contraction tracks
- Main-sequence evolution

These models are correct for equilibrium physics.

Our work does not contradict classical models but rather addresses a different question: *How do systems reach the equilibrium states described by classical theory?*

Classical models implicitly assume:

- Steady or quasi-steady accretion
- Symmetric mass distribution
- Efficient angular momentum transport
- Moderate, symmetric feedback
- Isolation from external perturbations

These assumptions are appropriate for describing stars once they have achieved stability. They are less applicable to the turbulent, non-equilibrium, interaction-rich environments where stars form.

Binary systems provide the pathway from chaos to equilibrium.

9.2. *When Does Isolated Formation Succeed?*

We do not claim isolated star formation is impossible, only that it requires special conditions:

9.2.1. *Low-Density Environments*

In regions with $n < 10^4$ cm^{-3} (e.g., Taurus):

- Turbulent Mach numbers are lower ($\mathcal{M} \sim 2$–5)
- Fragmentation is suppressed
- Interaction rates are reduced
- Deuterium-burst kicks are less likely to eject protostars from clouds

Isolated formation becomes viable because the challenges identified in §3 are weakened.

Predicted binary fraction: ∼25% (vs. ∼57% in Orion-like regions).

9.2.2. *Anomalously Low Angular Momentum*

Systems with $j < 10^{20}$ cm^2 s^{-1} have centrifugal radii:

$$r_{\rm cent} < 10 \text{ au}, \tag{53}$$

small enough that viscous angular momentum transport can operate before fragmentation.

Frequency: Log-normal distribution of angular momenta suggests ∼10–15% of systems fall below this threshold.

9.2.3. *Rapid Feedback Truncation*

If radiative or mechanical feedback disperses the gas envelope before fragmentation completes:

$$t_{\rm feedback} < t_{\rm frag}, \tag{54}$$

the system may be "frozen" as a single object.

Conditions: Requires massive protostar ($M > 5M_\odot$) with strong radiation pressure, or unusually strong magnetic winds.

9.3. *Implications for Planetary System Formation*

If >90% of stars form in binary or multiple systems, then **most planetary systems initially form in binary environments.**

9.3.1. *The Solar System*

The Sun is currently isolated. But if binary formation is nearly universal, the Solar System may have had an early companion that was:

- Ejected via three-body interaction in the birth cluster
- Lost to wide-binary disruption by passing stars
- Captured temporarily then released

Testable implications:

1. **Kinematic archaeology:** The Sun's velocity relative to local standard of rest ($v \sim 13$ km/s) could reflect ejection kick.
2. **Outer Solar System architecture:** Wide, eccentric orbits of trans-Neptunian objects could reflect perturbations from early companion.
3. **Isotopic anomalies:** If early companion underwent asymmetric supernova, ejecta could have contributed short-lived radionuclides found in meteorites.

9.3.2. *Planet Formation in Binaries*

Circumbinary planets are observed around close binaries (e.g., Kepler-16, -34, -35, -38, -413).

If most stars experienced binary phases:

- Planetary system architectures may reflect early dynamical sculpting by companions
- Migration and eccentricity may be more common than predicted by isolated-disk models
- Hot Jupiters could form via binary-driven migration rather than disk migration alone

9.4. *Observational Challenges and Future Work*

9.4.1. *Completeness Corrections*

The single greatest uncertainty is observational completeness. Different surveys use different:

- Wavelengths (optical, NIR, submm, radio)
- Techniques (imaging, spectroscopy, photometry, interferometry)
- Resolution limits
- Sensitivity thresholds
- Distance ranges

Critical need: Uniform completeness modeling across surveys to enable meaningful comparisons.

Next-generation instruments:

- JWST NIRCam: ∼0.1 arcsec resolution, detecting close companions in nearby regions
- ALMA long-baseline: ∼5–10 au resolution at 140 pc
- Extremely Large Telescopes (ELT, TMT, GMT): ∼10 mas resolution with adaptive optics

9.4.2. *Long-Duration Simulations*

Our framework predicts specific persistence time ratios and equilibration timescales. Direct validation requires numerical simulations with:

Technical requirements:

- **Open boundaries:** Sustained mass inflow $\dot{M}_{\rm in} \sim 10^{-5} M_\odot$ yr^{-1} over > 0.5 Myr
- **Radiation-MHD:** Non-ideal MHD with radiation transport
- **Resolution:** $\Delta x < 1$ au within 100 au of sink particles
- **Duration:** > 0.5 Myr with output cadence $\Delta t < 10^3$ yr
- **Chemistry:** Deuterium burning and episodic accretion
- **Statistics:** > 100 sink particles across > 10 realizations

Key measurements:

1. Configuration residence time distributions: $P(\tau|C)$
2. Transition matrices: $\lambda_{C\to C'}(t)$
3. Mass exchange rates: $\dot{M}_{A\leftrightarrow B}(t)$
4. Separation evolution: $a(t)$ for individual binaries
5. Ejection velocity distributions
6. Circumbinary reservoir masses: $M_{\rm CB}(t)$

Such simulations are computationally expensive but within reach of current supercomputers (e.g., ORNL Summit, NERSC Perlmutter).

9.4.3. *Chemical Signatures*

If mass exchange homogenizes composition between binary components, abundance patterns should differ between:

- **Close binaries:** Similar [Fe/H], [α/Fe] in both stars
- **Wide binaries:** Independent enrichment histories, greater scatter
- **Singles:** Truncated accretion signatures (anomalous abundances)

Observational test: High-resolution spectroscopy of binary components vs. singles in same cluster.

9.5. *Extensions to Other Mass Regimes*

9.5.1. *Brown Dwarfs ($M < 0.08 M_\odot$)*

Do the same principles apply at substellar masses?

Key question: If hydrogen-burning threshold is not reached, does mass exchange still provide functional advantage?

Hypothesis: Yes, for deuterium burning. Binary brown dwarfs may sustain longer deuterium-burning phases through mass exchange, explaining observed luminosity functions.

Prediction: Binary fraction among young brown dwarfs should be similarly high (∼60–80%) but decline

more rapidly than stellar binaries due to weaker gravitational binding.

Current observations: Brown dwarf binaries are common (∼20–30% in field), but completeness corrections for close pairs are severe.

9.5.2. *Massive Stars ($M > 8M_\odot$)*

Massive star formation involves strong radiative feedback:

$$L \sim 10^4 L_\odot \Rightarrow \text{radiation pressure} \sim \text{gravity}. \quad (55)$$

Question: Does radiation pressure disrupt binaries or does binarity enable massive star formation?

Evidence for binarity enabling massive formation:

- Most massive stars ($M > 20M_\odot$) are in binaries/multiples
- Radiation pressure along polar axis can be channeled through disk
- Mass exchange can prevent radiation-driven dispersal of one component

Hypothesis: Binary configuration may be *even more essential* for massive stars, providing:

- Distributed feedback (two moderate sources vs. one extreme source)
- Continued gas supply through circumbinary reservoir
- Orbital energy sink for radiation pressure momentum

Prediction: Isolated massive star formation should be extremely rare; most $M > 10M_\odot$ stars should have close companions or show evidence of past binary interaction.

10. CONCLUSIONS

We have demonstrated that binary star formation plays a functional role in overcoming fundamental physical challenges inherent to protostellar evolution in realistic environments. The key findings are:

10.1. *Binary Systems Are Optimal for Star Formation*

Six mechanisms operate synergistically:

1. **Mass recycling:** Material ejected from episodic deuterium burning is gravitationally recaptured rather than lost, converting open systems into closed-loop configurations.
2. **Angular momentum redistribution:** Orbital angular momentum provides a large reservoir enabling efficient transport, overcoming centrifugal barriers on timescales $t_{\rm tidal} \sim 10^4$ yr vs. $t_{\rm visc} \sim 10^5$ yr in isolated systems.
3. **Orbital stability:** Momentum kicks from asymmetric explosions are absorbed into orbital eccentricity rather than spatial displacement, keeping systems in dense gas reservoirs.
4. **Enhanced capture:** Dual gravitational wells sweep 4–5× larger effective cross-sections than single objects, sustaining accretion in turbulent environments.
5. **Distributed feedback:** Luminosity distributed between two components reduces peak Eddington ratios and enables asynchronous burning phases that buffer against runaway instabilities.
6. **Mutual equilibration:** Feedback-coupled evolution drives both components toward similar $L/L_{\rm Edd}$ ratios through self-regulating mass exchange, achieving stable hydrogen burning without fine-tuning.

10.2. *Observational Incompleteness Hides True Binary Dominance*

Kepler's detection of >2500 eclipsing binaries represents only ∼10% geometric probability, implying >25,000 true binaries. Applying similar corrections:

- Observed Class 0/I: 60–70% binaries → **True: >90%**
- Observed field: 30–45% binaries → **True: ∼60%**

10.3. *Post-Formation Disruption Implies Near-Universal Initial Binary Formation*

Binary fractions decline by ∼30% over Gyr timescales due to three-body encounters, stellar evolution mass loss, Kozai-Lidov oscillations, and galactic tides. If 60% remain after 10 Gyr of disruption:

$$f_{\rm initial} \approx 90\text{–}95\% \quad (56)$$

Nearly all stars form in binary or multiple systems.

10.4. *Singles Result from Three Pathways*

Field single stars arise from:

- **Disrupted binaries (∼60–70%):** Three-body ionization, supernovae, mergers

- **Low-density formation (∼20–30%):** Taurus-like regions where challenges are weakened
- **Statistical outliers (∼5–10%):** Rare fine-tuned conditions

10.5. *Universal Principle: Coupling Provides Stability*

Binary dominance in star formation reflects a principle operating across physical scales:

- Cooper pairs enable superconductivity (10^{-9} m)
- DNA double helices enable genetic stability (10^{-9} m)
- Diploid chromosomes enable evolutionary robustness (10^{-6} m)
- Binary stars enable thermonuclear ignition (10^{11} m)
- Galaxy pairs enable structure formation (10^{22} m)

In each case, **coupling expands the stability region in parameter space**, converting systems requiring fine-tuning into self-regulating configurations.

10.6. *Control Theory Perspective*

From an engineering viewpoint, the choice is:

(A) Stabilize one open system with stochastic inputs (requires fine-tuning)

(B) Use two coupled systems with feedback (self-regulating)

Nature, like engineering, chooses option B.

10.7. *Implications*

(1) Star formation is binary formation. Classical single-star models remain valid for describing equilibrium states, but the pathway to equilibrium in realistic environments proceeds primarily through binary configurations.

(2) Planetary systems form in binary contexts. If >90% of stars experience binary phases, most planetary systems—including potentially our own Solar System—formed under conditions influenced by companions.

(3) Simulation requirements. Validating this framework requires long-duration (>0.5 Myr), high-resolution (<1 au), open-boundary radiation-MHD simulations tracking configuration residence times.

(4) Observational priorities. Completeness-corrected multiplicity surveys across evolutionary stages and environments, combined with kinematic, chemical, and disk morphology studies, can test the six predictions enumerated in §6.

10.8. *Final Statement*

We conclude that binary star formation is not merely common but **optimal**. In the turbulent, magnetized, non-equilibrium conditions characteristic of molecular clouds, binary systems with orbital mass exchange provide the physical solution to achieving stable thermonuclear equilibrium.

The dominance of binaries is not coincidental but functional—it reflects fundamental physics favoring coupled, self-regulating systems over isolated configurations requiring fine-tuning.

Star formation through binarity is nature's engineering solution to the stabilization problem.

I thank colleagues for discussions that shaped these ideas and anonymous reviewers whose critiques will undoubtedly strengthen this work. This research made use of NASA's Astrophysics Data System and the arXiv preprint repository.

REFERENCES

Audard, M., et al. 2014, Protostars and Planets VI, 387

Baraffe, I., et al. 2009, ApJL, 702, L27

Bate, M. R. 2012, MNRAS, 419, 3115

Crutcher, R. M. 2012, ARA&A, 50, 29

Duchêne, G., & Kraus, A. 2013, ARA&A, 51, 269

Dunham, M. M., et al. 2014, Protostars and Planets VI, 195

Hayashi, C. 1961, PASJ, 13, 450

Hennebelle, P., & Inutsuka, S. 2019, Front. Astron. Space Sci., 6, 5

Iben, I. 1965, ApJ, 141, 993

Kirk, B., et al. 2016, AJ, 151, 68

Moe, M., & Di Stefano, R. 2017, ApJS, 230, 15

Offner, S. S. R., et al. 2022, in Protostars and Planets VII, arXiv:2203.10066

Palla, F., & Stahler, S. W. 1999, ApJ, 525, 772

Stahler, S. W. 1988, ApJ, 332, 804

Tobin, J. J., et al. 2022, ApJ, 925, 39

Tohline, J. E. 2002, ARA&A, 40, 349